Physics and Imaging in Radiation Oncology 11 (2019) 92–97

Contents lists available at ScienceDirect

Physics and Imaging in Radiation Oncology

journal homepage: www.elsevier.com/locate/phro

Original Research Article

Dose to medium in head and neck radiotherapy: Clinical implications for target volume metrics

Nicholas Hardcastle[a,b,*], Atousa Montaseri[a], Jenny Lydon[a], Tomas Kron[a,c], Glen Osbourne[d], Georgina Casswell[e], David Taylor[a], Lisa Hall[d], Lachlan McDowell[e,c]

[a] Physical Sciences, Peter MacCallum Cancer Centre, 305 Grattan St, Melbourne, Victoria 3000, Australia
[b] Centre for Medical Radiation Physics, University of Wollongong, Wollongong, NSW 2522, Australia
[c] Sir Peter MacCallum Department of Oncology, The University of Melbourne, Victoria, Australia
[d] Department of Radiation Therapy, Peter MacCallum Cancer Centre, 305 Grattan St, Melbourne, Victoria 3000, Australia
[e] Department of Radiation Oncology, Peter MacCallum Cancer Centre, 305 Grattan St, Melbourne, Victoria 3000, Australia

ARTICLE INFO

Keywords:
Dose to medium
Acuros
Dose calculation
IMRT
Head and neck cancer
Linear boltzman transport equation

ABSTRACT

Background and purpose: In radiotherapy dose calculation, advanced type-B dose calculation algorithms can calculate dose to medium (D_m), as opposed to Type-B algorithms which compute dose to varying densities of water (D_w). We investigate the impact of D_m on calculated dose and target coverage metrics in head and neck cancer patients.

Methods and materials: We reviewed 27 successfully treated (disease free at two-years post-(chemo)radiotherapy) human papillomavirus-associated (HPV) oropharyngeal cancer (ONC) patients treated with IMRT. Doses were calculated with Type-B and Linear Boltzman Transport Equation (LBTE) algorithms in a commercial treatment planning system, with the treated multi-leaf collimator patterns and monitor units. Coverage for primary Gross Tumour Volume (GTVp), high dose Planning Target Volume (PTV) (PTV_High), mandible within PTV_High (Mand ∩ PTV) and PTV_High excluding bone (PTV-bone) were compared between the algorithms.

Results: Dose to 95% of PTV_High with LBTE was on average 1.1 Gy/1.7% lower than with Type-B (95%CI 1.5–1.9%, $p < 0.0001$). This magnitude was inversely linearly correlated with the relative volume of the PTV_High containing bone (pearson $r = -0.81$). Dose to 98% of the GTVp was 0.9 Gy/1.3% lower with LBTE compared with Type-B (95%CI 1.1–1.5%, $p < 0.05$). Dose to 98% of Mand ∩ PTV was on average 3.4 Gy/5.0% lower with LBTE than with Type-B (95%CI 4.6–5.4%, $p < 0.0001$).

Conclusion: In OPC treated with IMRT, D_m results in significant reductions in dose to bone in high dose PTVs. Reported GTVp dose was reduced, but by a lower magnitude. Reduced coverage metrics should be expected for OPC patients treated with IMRT, with dose reductions limited to regions of bone.

1. Introduction

Dose calculation algorithms in contemporary radiation therapy are typically model based, where a beam model is used to calculate the fluence entering the patient through modelling of the components of the delivery system [1]. Following calculation of incident fluence, a dose calculation algorithm then calculates particle transport and deposited energy in the patient [1,2]. Energy deposition varies in complexity with respect to heterogeneities in patient composition and their impact on primary and scattered photon and electron fluence. Type B algorithms, which take into account the effect of heterogeneities on primary and scattered photons and electrons [3], typically report dose to water (D_w), as the electron deposition kernels/equations are calculated based on water of varying densities [2]. Variation exists in the calculation of primary attenuation based on material specific attenuation coefficients used, leading to Type B algorithms reporting either purely D_w, or a combination of D_w and dose to medium (D_m) [4]. More advanced Type B algorithms (Monte Carlo and deterministic solving of the linear Boltzmann transport equations (LBTE)) however, calculate the transport of photons and electrons within the specific media assigned from the CT, and then compute energy deposition within specific materials, thus can inherently report D_m [2]. In the case of Monte Carlo, D_m is inherently computed, and to achieve D_w, the stopping power ratios between the medium and water are used. In the case of the LBTE, the energy fluence is computed in each voxel, but deposition of dose is computed by multiplication of the electron fluence

* Corresponding author at: Physical Sciences, Peter MacCallum Cancer Centre, 305 Grattan St, Melbourne 3000, VIC, Australia.
E-mail address: nick.hardcastle@petermac.org (N. Hardcastle).

https://doi.org/10.1016/j.phro.2019.08.005
Received 2 June 2019; Received in revised form 21 August 2019; Accepted 28 August 2019

spectrum by the energy deposition cross section (restricted electron stopping power for the medium) integrated over energy, divided by the mass density at the given location. Therefore D_m, within the specific medium, or D_w, within the specific medium is inherently reported [5].

The dosimetric accuracy of LBTE has been investigated for a range of materials and treatment geometries and techniques [6–9], the findings generally indicating improved accuracy of the LBTE algorithm over Type B algorithms. The impact of reporting to D_w and D_m has been discussed for lung [10–12], breast [13], bone [14,15] and head and neck [16–18]. Recommendations have also been made for reporting dose in the routine clinical setting and in clinical trials [4,19] in the context of both Monte Carlo and LBTE algorithms. The dosimetric impact of using LBTE in head and neck cancer (HNC) has been investigated for nasopharyngeal carcinoma [20–22], showing overall typically 1% lower doses in tissue, but up to a 4% reduction in dose to bone lying within the target volume, which could be part of clinical target volume (CTV) due to bone invasion or merely a result of a geometric expansion for planning target volume (PTV) creation. These studies have not made any link with clinical outcome of the patients, therefore the clinical impact of these deficiencies in dose coverage are unknown. These results are largely consistent with planning studies in other anatomical sites, where dose to soft tissues including muscle is usually 1–2% lower with LBTE compared with a Type B algorithm reporting D_w [13].

The dosimetric differences observed when transitioning to an LBTE algorithm reporting D_m, in the absence of clinical data, pose a clinical conundrum. Either accept potential reductions in reported dose coverage and provoke anxiety with potential loss of tumour control probability, or maintain previous target volume coverage recommendations resulting in potential increased dose to adjacent normal tissue. In this context, we conducted a retrospective planning study in successfully treated HPV-OPC patients using a commercial LBTE algorithm reporting D_m. Newly calculated dose distributions were compared to the parameters accepted on previously utilised plans in order to inform on target coverage dose constraints required with LBTE. To our knowledge, this is the first time the dosimetric impact of transitioning to an advanced Type B algorithm reporting D_m has been tied to clinical outcomes.

2. Materials and methods

A cohort of 27 previously treated HPV-OPC patients were selected for analysis. Patient characteristics are provided in Supplementary Table 1. All patients were disease-free with at least two years follow up after completion of definitive (chemo)radiotherapy. The treatment plans that resulted in disease control were recalculated using AcurosXB D_m (AXB Varian Medical Systems, Palo Alto, USA). Our institutional practice at the time was a split neck technique, consisting of an upper neck field treated with a sliding-window IMRT technique (5–9 beams), junctioned with an elective lower neck field of 2–3 anterior-posterior 3DCRT fields [23]. All patients were planned in Eclipse and dose was calculated with Anisotropic Analytical Algorithm v11.0 (AAA, Varian Medical Systems, Palo Alto, USA).

For each patient, a duplicate of the treatment planning CT and structure set was created. The physical material table was set to AcurosXB v13.5; the mapping from CT Hounsfield Units to physical materials is discussed in the supplementary material. All structures of interest were reviewed for consistency of nomenclature. The primary structures of interest were the primary GTVs (GTVp) and the high dose PTV (PTV_high; prescription dose 70 Gy). We created two additional structures: (1) mandible within the PTV_high ('mand ∩ PTV'); and (2) PTV_high excluding mandible ('PTV-mand'). The cartilage/bone was defined using an automated threshold of 120 HU/1.10 gcm^{-3}. The original treatment plan including all IMRT and 3DCRT fields were copied to the duplicate data set and the original monitor units and MLC motions retained for each field. The dose distribution was calculated with both AAA v15.5 and AXB v15.5 (AXB v15.5), D_m. These models were both created based on the same measured beam data and use the same MLC parameters (dosimetric leaf gap and transmission). The vendor recommended source sizes were used; 1 mm (X) and 0 mm (Y) for AAA and 1.5 mm (X) and 0 mm (Y) for AXB, where X is the direction of leave travel and Y is the direction orthogonal to this. We chose not to evaluate AXB D_w, as international recommendations are to avoid use of D_w when using Monte Carlo or LBTE [4,19,24].

To evaluate the effect of D_w and D_m between the algorithms for various materials to provide context for the patient plans, a $50 \times 50 \times 50\,cm^3$ water phantom was created and a $2 \times 2 \times 2\,cm^3$ cube placed at a depth of 10 cm. A $5 \times 5\,cm^2$ 6 MV photon field was placed incident on the phantom. The cube material was set to air (HU = -1000), water (HU = 0), adipose tissue (HU = -100), skeletal muscle (HU = 35), cartilage (HU = 103) or bone (HU = 1192), and the dose from AAA v15.5 and AXB v15.5 was calculated for the same number of MU for each material setting. The difference in dose at the centre of the heterogeneity cube was compared between algorithms.

The Eclipse Scripting API extracted dosimetric data from the original plan (calculated with AAA v11.0) and the recalculated plans using AAA v15.5 and AXB v15.5. To ensure differences in calculated dose was limited to algorithmic differences, the metrics were compared between the two AAA versions to determine consistency of the current model with historical version and beam models. The following parameters were compared between algorithms: (1) Dose to 98% (D98%) of the GTVp, (2) Dose to 95% (D95%) of the PTV_high, (3) near maximum dose (D2%) of the PTV_high, (4) dose to 98% of the mandible within the high dose PTV (mand ∩ PTV) and dose to 95% of the high dose PTV, excluding bone and cartilage (PTV-Bone). We further evaluated the change in dose to 95% of the high dose PTV as a function of the proportion of bone within this contour. The doses to intermediate and low dose PTVs were not evaluated in this study due to the much lower bone proportion. To further elucidate any change in dose between algorithms relative to the target and OAR anatomy, for a representative patient the isocentre was shifted in 3 mm in each direction and the dose recalculated.

Differences in dosimetric metrics between algorithms were evaluated using Estimation Statistics [25]. The metric of interest was displayed for each patient using swarm plots, with each patient's data for both algorithms displayed using a line joining the two algorithms. The distribution on the right of each plot shows the confidence interval of the difference in the means, with the zero location of this axis aligned with the mean of the control algorithm.

3. Results

There was a statistically significant but clinically insignificant difference between the plans calculated with AAA v11.0 (original treatment plans) and AAA v15.5 (supplementary data), therefore we present AAA v15.5 for all comparisons with AXB v15.5 to ensure differences are purely due to the dose calculation algorithm rather than beam modelling differences. For a single incident beam on a water phantom with a cube of varying materials, the dose in the centre of the cube with AAA v15.5 was greater than that calculated with AXB v15.5 by 0.2% (adipose tissue), 0.5% (water), 1.3% (skeletal muscle), 1.3% (cartilage), 4.9% (bone) and 10.1% (air).

For a representative patient, the reduced 95% isodose coverage in the region of bone when using AXB v15.5 is clearly visible (Fig. 1). With AXB v15.5, the mean GTVp_High D98% was reduced by 1.3% (95% CI 1.1–1.5%, $p < 0.05$), compared with AAA v15.5 (Fig. 2 and Table 1). Further, with AXB v15.5 the PTV_High D95% was reduced by a mean of 1.7% (95% CI 1.5–1.9%, $p < 0.0001$) and the PTV_High D2% was reduced by a mean of 0.5% (95% CI 0.3–0.8%, $p < 0.05$) compared with AAA v15.5 (Fig. 2 and Table 1).

The dose to the PTV_High with bone removed was evaluated, as was the dose to the mandible overlapping with the PTV_High. The dose to

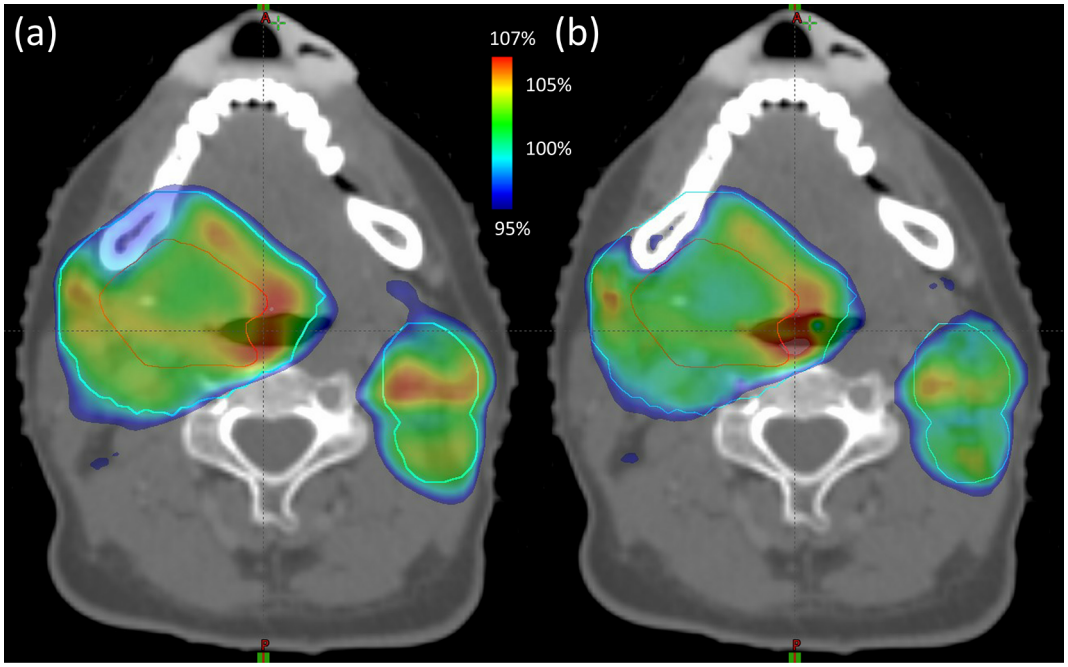

Fig. 1. Example patient showing the 95% prescription dose coverage and the GTVp (red) and PTV (cyan) for (a) AAA v15.5 and (b) AXB v15.5. Note the reduced dose in the mandible within the PTV. (For interpretation of the references to colour in this figure legend, the reader is referred to the web version of this article.)

95% of the PTV_High without bone was reduced by a mean of 1.1% (95% CI 1.0–1.3% Gy, $p < 0.001$) with AXB v15.5 compared with AAA v15.5 (Fig. 3 and Table 1). The dose to 98% of the mandible overlapping with PTV_High was however reduced on average by 5.0% (95% CI 4.6–5.4% Gy, $p < 0.0001$) when calculated with AXB v15.5, compared with AAA v15.5 (Fig. 3 and Table 1). These differences are broadly consistent with that calculated in the phantom geometry.

The reduction in the dose to 95% of the PTV_High was plotted as a function of the proportion of this volume that consisted of cartilage or bone; As the proportion of cartilage/bone within the PTV_high increases, there was a corresponding decrease in PTV_High coverage (pearson correlation coefficient = −0.81) (Fig. 4). For a representative patient, when the isocentre position was varied, the cold spot maintained its position on the mandible (Fig. 5). The static location of the cold spot in the PTV highlights the dose reduction is due to D_m calculated in bone, rather than beam fluence.

4. Discussion

The increases in calculation speed and improvements in algorithm efficiency have facilitated the use of advanced Type B algorithms such as Monte Carlo and LBTE in routine radiotherapy treatment planning. While the evolution of dose calculation algorithms provides improved accuracy, it can also present a very real challenge to the clinicians during the implementation phases, particularly where there are significant differences in target volume coverage. In the current study, we have quantified the effect observed in our head and neck IMRT plans, demonstrating clinically significant variations in standard dosimetry metrics as a result of a switch from a Type B to an advanced Type B dose calculation algorithm which reports D_m.

Our results show that for the same monitor units and MLC patterns, recalculating these with a LBTE algorithm with D_m resulted in a reduction in dose to both the soft tissue (by approximately 1%) and bone (by approximately 5%) component within the high dose PTV. We have

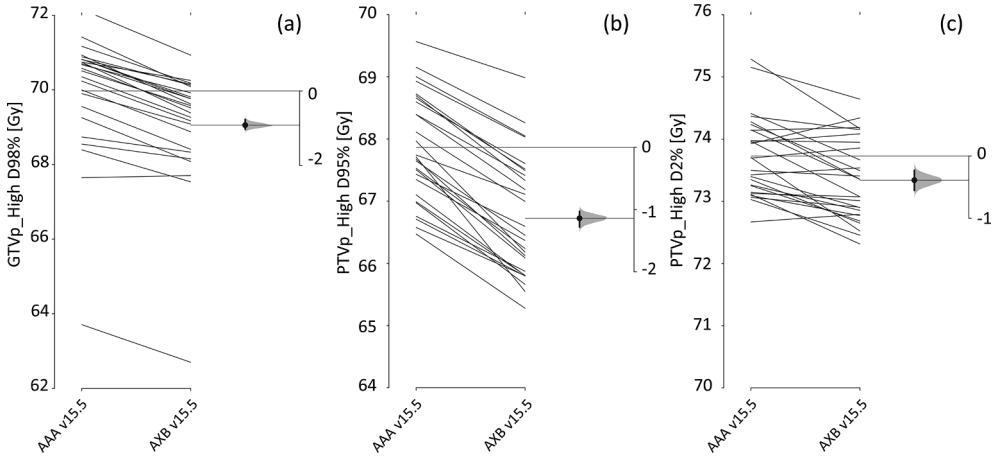

Fig. 2. Comparison of (a) GTVp_High D98%, (b) PTV_High D95% and (c) PTV_High D2% between AAA v15.5 and AXB v15.5.

Table 1
Calculated metrics for target and mandible structures of interest. The p value was calculated using a Wilcoxon signed rank test.

Structure	Metric	AAA v15.5 (Gy)	AXB v15.5 (Gy)	Mean Difference (Gy/%)	*95% confidence interval (Gy/%)*	*p*
GTVp_High	D98%	69.97 ± 1.67	69.06 ± 1.58	−0.92/−1.3%	−1.0 – −0.8/−1.1–1.5	p < 0.05
PTV_High	D95%	67.86 ± 0.86	66.73 ± 0.97	−1.13/−1.7%	−1.3 – −1.0/−1.5 – −1.9	p < 0.0001
	D2%	73.72 ± 0.65	73.34 ± 0.65	−0.38/−0.5%	−0.6 – −0.2/−0.3 – −0.8	p < 0.05
mand ∩ PTV	D98%	67.32 ± 0.98	63.94 ± 0.96	−3.38/−5.0%	−3.6 – −3.1/−4.6 – −5.4	p < 0.0001
PTV-bone	D95%	67.02 ± 0.87	67.24 ± 0.88	−0.77/−1.1%	−0.8 – −0.7/−1.0 – −1.3	p < .001

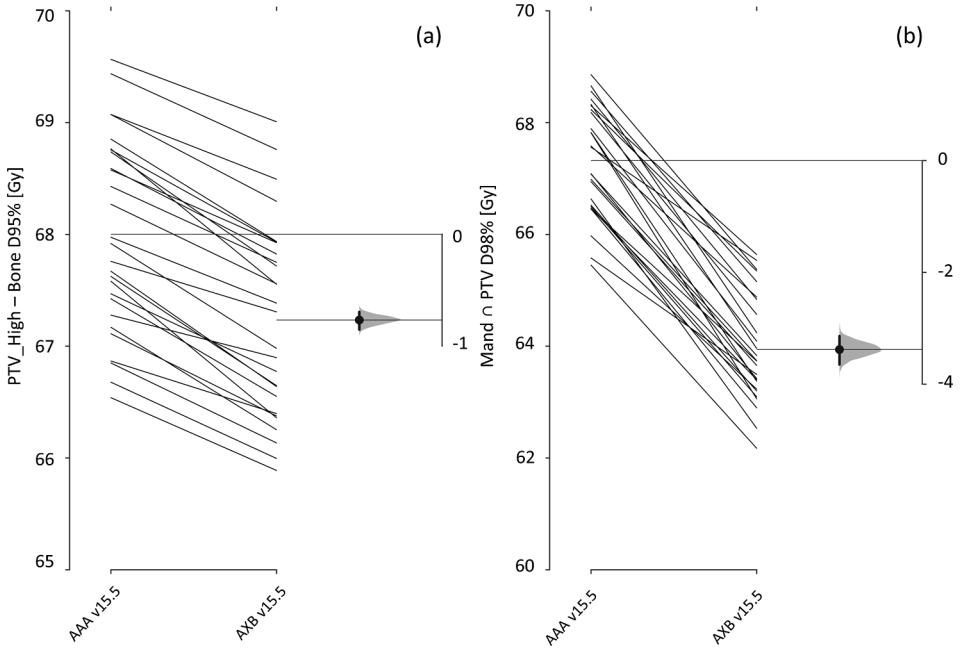

Fig. 3. (a) Dose to 95% of the PTV_High excluding bone b) and dose to 98% of the mandible within the PTV_High volume.

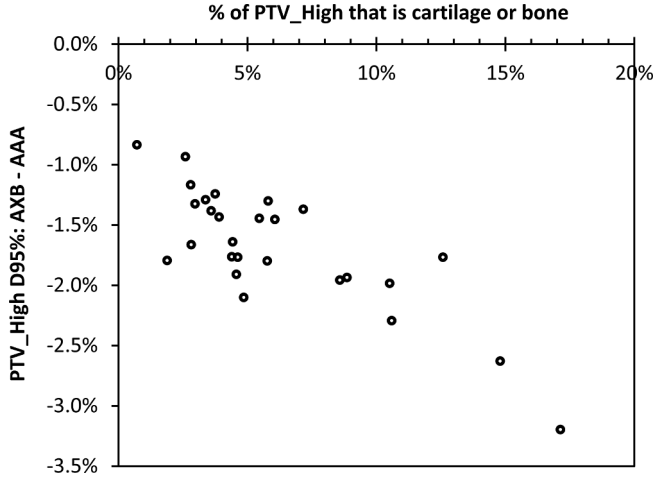

Fig. 4. Change in D95% for the high dose PTV as a function of the percentage of the PTV that is cartilage or bone.

also shown that this cold spot is limited to the bone, as it does not move with isocentre shifts. These results are consistent with that observed by Dogan et al. for Monte Carlo calculation [18], and by others investigating LBTE in head and neck cancers [20–22]. Importantly, in the current study we selected HPV + oropharyngeal cancer patients with no evidence of recurrence, all of whom were at least two years post-radiotherapy. The incorporation of long-term clinical follow up into this study is reassuring, as all these patients were treated with lower than appreciated doses at the time of plan acceptance, and all achieved locoregional cure. While HPV-OPC could be seen as 'low-hanging fruit' for this project, given 70 Gy may be in excess of what is needed, this cohort was selected, because accepting any increase in dose is contrary to the current research efforts and even small increases in dose can have significant implications for acute and long term toxicity in the doses used in HNC. It is acknowledged however that this is not a comprehensive clinical analysis, as we have not included patients with locoregional failure. This should be further tested with a larger sample size that includes patients with both locoregional control and failure.

Fig. 4 highlights that the variation in the expected covering isodose difference moving from dose calculation algorithms reporting D_m instead of D_w is patient specific, and depends on the component of the PTV that is bone. Not taken into account in this figure is the proportion of the PTV that is in air. LBTE calculated a lower dose in air compared with AAA by 10% in the phantom calculation, therefore some deviation from a clear trend line may be due to the air component in the PTV. It is fundamental however that any dose reduction is contained in the bone components of the target; any modification of target coverage goals in the planning process should be scrutinised to ensure the location of the dose deficit is within bone.

The reduced dose to mandible shown in this study also suggests that the threshold for mandibular osteoradionecrosis must be taken in the context of the dose calculation algorithm. If D_m is used, the constraint may be lower than the previously recommended dose thresholds using D_w. There is also potential for optimisation algorithms to attempt to increase dose to colder components of the target volume; this may result in increases in the dose to mandible above that which was previously observed, and a consequential increase in the risk of osteoradionecrosis. Therefore any attempt to increase target coverage to levels previously attained with D_w based algorithms must be made with

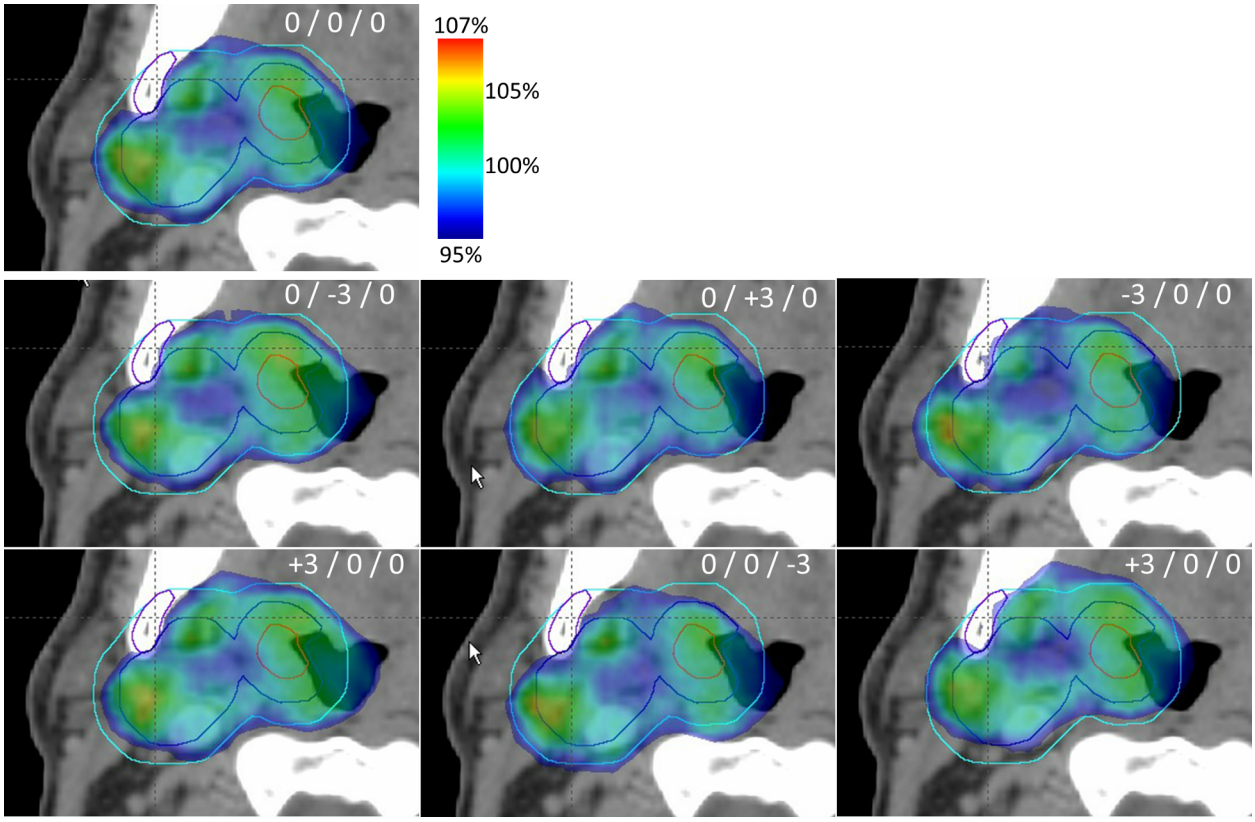

Fig. 5. Change in 95% isodose line with shifts of 3 mm in each direction (LR/SI/AP). The cyan contour is PTV_High, the blue is CTV_High and the red is GTVp_High. (For interpretation of the references to colour in this figure legend, the reader is referred to the web version of this article.)

extreme caution [26].

While the differences to soft tissue appear relatively small, we observed an impact on clinical dosimetry metrics in HNC treatment plans. This requires the radiation oncologist to either continue to use conventional minimum target volume coverage recommendations based on D_w algorithms, or accept lower target volume coverage with the D_m algorithm. Without comparative clinical data, this poses a clinical conundrum; the former resulting in potential increased dose to normal tissue, while the latter provoking anxiety with a potential loss in tumour control probability. This is particularly relevant in HNC owing to both the number of complex tissue interfaces and the narrow therapeutic index. Accepting even small increases in the delivered radiation dose in HNC plans has the potential for a more-than-linear increase in toxicity given the slope of the dose response curve for some of the organs at risk in this dose region. In HNC, this is particularly pertinent to patients with human papillomavirus-associated oropharyngeal cancer (HPV-OPC) and accepting any increase is contrary to the considerable research efforts currently underway to find an appropriate treatment de-escalation schedule.

The achievable target coverage and bone OAR metrics from the change in algorithm from D_w to D_m has implications on clinical trial dosimetry. In current radiation therapy practice there is variation in the algorithm reporting mode. This will result in variation of achievable dosimetry between centres using different reporting mechanisms, as well as variation in the actual dose received by the patients enrolled in different centres. Despite recommendations by Ma et al. [19] and Gladstone et al. [4] who recommend to report D_m if this is inherently reported, (instead of D_w which has been converted from D_m), or D_w if this is what is inherently reported, there will still be residual variation between algorithms inherently calculating D_m or D_w. This is particularly of note for the LBTE algorithm evaluated here, which can inherently calculate either D_m or D_w in the medium of interest. As more centres convert to D_m algorithms awareness of the dosimetric changes is important to reduce potential over-treatment of patients, particularly in the era of a large proportion of patients being treated for HPV + tumours.

The limitations of this comparative planning study are its small size and applicability to the cohort it was studied in. Currently, there is much research effort aimed at treatment de-escalation in HPV-associated oropharyngeal cancer and it is possible that the dose threshold for cure may be substantially lower for the majority of patients than was used in this study. However, the corresponding argument for the applicability of these results are quite clear: in a patient cohort with excellent locoregional control, there is no rationale to accept higher doses with new planning algorithms, as the potential for long term harm will increase.

In oropharyngeal cancer patients who were free from local failure treated with IMRT, the dose calculated with AcurosXB D_m is in general lower than that calculated by AAA algorithm by 1% in tissue and up to 5% in bone. This has implications on achievable target coverage and dose to bone OAR metrics and is clinically important for planning optimization and clinical trial reporting. When using AcurosXB D_m, lower target coverage metrics are likely required compared with when using AAA; these must be carefully reviewed to ensure dose deficits are limited to bone.

Acknowledgement

The Peter MacCallum Cancer Centre Foundation for support for this research.

Declaration of Competing Interest

We wish to confirm that there are no known conflicts of interest associated with this publication and there has been no significant financial support for this work that could have influenced its outcome.

NH and TK report grant funding from Varian Medical Systems for an unrelated project.

Appendix A. Supplementary data

Supplementary data to this article can be found online at https://doi.org/10.1016/j.phro.2019.08.005.

References

[1] Mackie RT, Liu HH ME. Treatment planning algorithms: model-based photon dose calculations. In: Kahn FM, Gerbi BJ, editors. Treat. Plan. Radiat. Oncol., Philadelphia: Lippincott Williams and Wilkins; 2012, p. 93–109.

[2] 4. Treatment Planning Algorithms. J Int Comm Radiat Units Meas 2014;14:65–75. doi:10.1093/jicru/ndx014.

[3] Knöös T, Wieslander E, Cozzi L, Brink C, Fogliata A, Albers D, et al. Comparison of dose calculation algorithms for treatment planning in external photon beam therapy for clinical situations. Phys Med Biol 2006;51:5785–807. https://doi.org/10.1088/0031-9155/51/22/005.

[4] Gladstone DJ, Kry SF, Xiao Y, Chetty IJ. Dose Specification for NRG Radiation Therapy Trials. Int J Radiat Oncol Biol Phys 2016;95:1344–5. https://doi.org/10.1016/j.ijrobp.2016.03.044.

[5] Vassiliev ON, Wareing TA, McGhee J, Failla G, Salehpour MR, Mourtada F. Validation of a new grid-based Boltzmann equation solver for dose calculation in radiotherapy with photon beams. Phys Med Biol 2010;55:581–98. https://doi.org/10.1088/0031-9155/55/3/002.

[6] Vassiliev ON, Wareing TA, McGhee J. Validation of a new grid-based Boltzmann equation solver for dose calculation in radiotherapy with photon beams. Phys Med Biol 2010;55:581–98.

[7] Fogliata A, Nicolini G, Clivio A, Vanetti E, Cozzi L. Dosimetric evaluation of Acuros XB Advanced Dose Calculation algorithm in heterogeneous media. Radiat Oncol 2011;6. https://doi.org/10.1186/1748-717X-6-82.

[8] Han T, Mourtada F, Kisling K, Mikell J, Followill D, Howell R. Experimental validation of deterministic Acuros XB algorithm for IMRT and VMAT dose calculations with the Radiological Physics Center's head and neck phantom. Med Phys 2012;39:2193–202. https://doi.org/10.1118/1.3692180.

[9] Kang SW, Chung JB, Lee JW, Kim MJ, Kim YL, Kim JS, et al. Dosimetric accuracy of the Acuros XB and Anisotropic analytical algorithm near interface of the different density media for the small fields of a 6- MV flattening-filter-free beam. Int J Radiat Res 2017;15:157–65. https://doi.org/10.18869/acadpub.ijrr.15.2.157.

[10] Huang B, Wu L, Lin P, Chen C. Dose calculation of Acuros XB and Anisotropic Analytical Algorithm in lung stereotactic body radiotherapy treatment with flattening filter free beams and the potential role of calculation grid size. Radiat Oncol 2015;10. https://doi.org/10.1186/s13014-015-0357-0.

[11] Wang S, Li X, Zheng D, Zhen W, Zvolanek K, Hyun M, et al. A comprehensive dosimetric study on switching from a Type-B to a Type-C dose algorithm for modern lung SBRT. Radiat Oncol 2017;12. https://doi.org/10.1186/s13014-017-0816-x.

[12] Saiful Huq M, Hu B, Wynn R, Bednarz G, Combine AG, Lalonde RJ, et al. Clinical implementation and evaluation of the Acuros dose calculation algorithm. J Appl Clin Med Phys 2017;18:195–209. https://doi.org/10.1002/acm2.12149.

[13] Fogliata A, Nicolini G, Clivio A, Vanetti E, Cozzi L. On the dosimetric impact of inhomogeneity management in the Acuros XB algorithm for breast treatment. Radiat Oncol 2011. https://doi.org/10.1186/1748-717X-6-103.

[14] Sterpin E, Palmans H, Reynaert N, Crop F, Kawrakow I. On the conversion of dose to bone to dose to water in radiotherapy treatment planning systems. Phys Imaging Radiat Oncol 2018;5:26–30. https://doi.org/10.1016/j.phro.2018.01.004.

[15] Miura H, Shiomi H, Oh R-J, Inoue T, Masai N, Usmani MN, et al. Comparison of Absorbed Dose to Medium and Absorbed Dose to Water for Spine IMRT Plans Using a Commercial Monte Carlo Treatment Planning System. Int J Med Physics, Clin Eng Radiat Oncol 2014;03:60–6. https://doi.org/10.4236/ijmpcero.2014.31010.

[16] Muñoz-Montplet C, Marruecos J, Buxó M, Jurado-Bruggeman D, Romera-Martínez I, Bueno M, et al. Dosimetric impact of Acuros XB dose-to-water and dose-to-medium reporting modes on VMAT planning for head and neck cancer. Phys Medica 2018;55:107–15. https://doi.org/10.1016/j.ejmp.2018.10.024.

[17] Kan MWK, Leung LHT, Yu PKN. Verification and dosimetric impact of Acuros XB algorithm on intensity modulated stereotactic radiotherapy for locally persistent nasopharyngeal carcinoma. Med Phys 2012;39:4705–14. https://doi.org/10.1118/1.4736819.

[18] Dogan N, Siebers JV, Keall PJ. Clinical comparison of head and neck and prostate IMRT plans using absorbed dose to medium and absorbed dose to water. Phys Med Biol 2006;51:4967–80. https://doi.org/10.1088/0031-9155/51/19/015.

[19] Ma CM, Li J. Dose specification for radiation therapy: Dose to water or dose to medium? Phys Med Biol 2011;56:3073–89. https://doi.org/10.1088/0031-9155/56/10/012.

[20] Hirata K, Nakamura M, Yoshimura M, Mukumoto N, Nakata M, Ito H, et al. Dosimetric evaluation of the Acuros XB algorithm for a 4 MV photon beam in head and neck intensity-modulated radiation therapy. J Appl Clin Med Phys 2017;16:52–64. https://doi.org/10.1120/jacmp.v16i4.5222.

[21] Kan MWK, Leung LHT, So RWK, Yu PKN. Experimental verification of the Acuros XB and AAA dose calculation adjacent to heterogeneous media for IMRT and RapidArc of nasopharygeal carcinoma. Med Phys 2013;40. https://doi.org/10.1118/1.4792308.

[22] Kan MWK, Leung LHT, Yu PKN. Dosimetric impact of using the acuros XB algorithm for intensity modulated radiation therapy and rapidarc planning in nasopharyngeal carcinomas. Int J Radiat Oncol Biol Phys 2013;85:e73–80. https://doi.org/10.1016/j.ijrobp.2012.08.031.

[23] Fua TF, Corry J, Milner AD, Cramb J, Walsham SF, Peters LJ. Intensity-modulated radiotherapy for nasopharyngeal carcinoma: clinical correlation of dose to the pharyngo-esophageal axis and dysphagia. Int J Radiat Oncol Biol Phys 2007;67:976–81. https://doi.org/10.1016/j.ijrobp.2006.10.028.

[24] Andreo P. Dose to "water-like" media or dose to tissue in MV photons radiotherapy treatment planning: Still a matter of debate. Phys Med Biol 2015;60:309–37. https://doi.org/10.1088/0031-9155/60/1/309.

[25] Ho J, Tumkaya T, Aryal S, Choi H, Claridge-Chang A. Moving beyond P values: Everyday data analysis with estimation plots. BioRxiv 2018;377978. https://doi.org/10.1101/377978.

[26] Chaikh A, Ojala J, Khamphan C, Garcia R, Giraud JY, Thariat J, et al. Dosimetrical and radiobiological approach to manage the dosimetric shift in the transition of dose calculation algorithm in radiation oncology: How to improve high quality treatment and avoid unexpected outcomes? Radiat Oncol 2018;13:1–11. https://doi.org/10.1186/s13014-018-1005-2.